



On buckling strength of cylindrical shells with openings under seismic loads

Fukuyoshi H.⁽¹⁾, Yoguchi H.⁽¹⁾, Murakami T.⁽¹⁾, Jimbo M.⁽¹⁾, Nakamura H.⁽²⁾, Matsuura S.⁽²⁾

(1) Toshiba Corporation, Japan

(2) Central Research Institute of Electric Power Industry, Japan

ABSTRACT: A series of static and dynamic buckling tests for cylindrical shells with openings under transverse shearing loads was carried out. Occurrence of buckling for dynamic and static tests were observed as ligaments were deformed in the radial direction. Response reduction factor estimated by the seismic buckling design guideline for cylindrical shells without opening was applied to the cylinders with openings, and it was determined that estimation by above method was conservative enough for the structure with openings.

1 INTRODUCTION

The Demonstration Test and Research Program of Buckling of LMFBR, commissioned by the Ministry of International Trade and Industry (MITI), was conducted by Central Research Institute of Electric Power Industry (CRIEPI) and the nuclear power plant manufacturers in Japan. The purpose of this program was to establish buckling design guides for LMFBR components under seismic loads. In the guide, in order to prevent elastic-plastic buckling, the concept of response reduction factor (D_s) was introduced to evaluate strength under seismic loads based on various buckling tests and analyses for cylindrical shells without openings[1]. Cylindrical shells with openings were planned to be used for the intermediate heat exchanger (IHX) of the Demonstration Fast Breeder Reactor (DFBR). Assuming that a main frame of IHX is subjected to infrequent severe seismic loads, the thickness should be greater, though greater thickness invites increased thermal stress. Therefore, investigation on buckling of cylinder with openings was carried out throughout static buckling tests[2], while buckling characteristics under dynamic loads has never been studied.

In this paper, a series of dynamic and static buckling tests under transverse shearing seismic loads was carried out and basic buckling characteristics for cylindrical shells with openings were clarified. D_s applied to cylindrical shells without opening was tried to introduce the structure with openings and discussed.

2 RESPONSE REDUCTION FACTOR

Considering the high ductility of austenitic stainless steel under alternative dynamic loads to structures, it is reasonable to take account of nonlinear deformation for structural integrity assessment under seismic loads. Linear response analysis is convenient and useful for calculating maximum load under seismic accelerations. In the event that large plastic energy absorption is caused, imaginary load evaluated by linear response analysis under seismic accelerations is larger than actual load. Therefore, in the seismic buckling design guide, a

response reduction factor was introduced.

If Q_e is imaginary load evaluated by linear response analysis under critical input acceleration to cause buckling, response reduction factor D_s is defined by the following equation;

$$D_s = \frac{Q_{cr}}{Q_e} \quad (1)$$

where Q_{cr} is actual buckling load. Accordingly, following equation was proposed to prevent plastic shear/bending buckling.

$$D_s Q_i < Q_{cr} \quad (2)$$

where Q_i is imaginary load evaluated by linear response analysis under design seismic loads.

In the present design guide based on many dynamic tests for cylindrical shells without openings, it is proposed that D_s is basically given from the equations below;

$$D_s = \frac{1}{\mu} \quad (3)$$

where μ is nonlinearity factor defined as;

$$\mu = \frac{\delta_{cr}}{\delta_e} \quad (4)$$

where δ_{cr} is actual transverse displacement when buckling occurs and δ_e is imaginary displacement when the elastic system's restoring force reaches the level of buckling load.

From the test results for cylindrical shells without openings, the following equation is proposed for estimating μ ;

$$\mu = 1 + 1.5 \exp(-8\lambda) \quad (5)$$

$$\lambda = \frac{S_y R}{E t} \quad (6)$$

where S_y is yield stress, E is Young's modulus, R and t are radius and thickness of cylinder, respectively.

3 TEST MODEL

A series of static and dynamic buckling tests under transverse shearing loads was carried out. Test models with radius(R) of 200mm and radius-to-thickness ratio(R/t) of 50 are shown in Fig.1. Openings were 110mm in height and 79.3mm in width. Aluminum alloy A3003P-O was used for the models to simulate mechanical properties of SUS304/316 under operating temperature of FBR.

Setups for dynamic and static tests are shown in Figs.2 and 3. Parameters for the tests were circumferential opening ratio, direction of loads, and loading amplitudes of max. input accelerations as shown in Table 1. Input acceleration time history and response spectrum of dynamic tests are shown in Fig.4. "ENVELOPE", simulated enveloped motion assumed in a half-embedded reactor building on a hard rock site, was adopted as seismic wave. It was filtered as in a building, and adjusted natural frequency of the models coincided with that of the designed DFBR. For each condition of dynamic tests, high-amplitude excitation was performed to cause buckling after low-amplitude excitations were performed. As for No.1-1, 2-1, and 3-1, the number of excitations were 6 or 7 and middle-amplitude excitations performing nonlinear response were contained.

4 TEST RESULTS

4.1 results of static tests

Results of load-displacement curves under static tests are shown in Fig.5. Comparing loading direction, buckling load in which loading direction was on the ligament side was larger than cases in which the loading direction was on the opening side. Examples of deformed models after repeated loads are shown in Fig.6. Occurrence of buckling was observed as ligaments were deformed in the radial direction. In the models, ligaments whose faces were almost beneath the loading axis were bulged, and others having faces almost parallel to the loading axis were shrunken in the radial direction. Therefore, a similar buckling mode was shown on each model.

4.2 results of dynamic tests

Examples of load-displacement curve and skeleton curves under seismic loads are shown in Figs.7 and 8.

For all the models, the tendency of deformed shapes coincided with the results of the above static tests. Buckling load under dynamic tests also coincided with those on corresponding conditions under static tests with errors of $\pm 5\%$ as shown in Table 2.

5 DISCUSSION

The relations between Q_{cr} / Q_i and δ / δ_{cr} under seismic loads are shown in Fig.9. No difference in circumferential opening ratio α was seen. Difference in loading direction was, however, shown as D_s , for which the loading direction was opening side, was larger than in cases where the loading direction was the loading side. This difference can be explained as plastic energy absorption. Plastic energy absorption which loading direction was the ligament side was larger than in cases where the loading direction was the opening side as shown in Fig.5.

The results of the tests and estimated response reduction factor D_s are shown in Table 3. D_s estimated by Eq (3) and (5) was 0.45. Experimental results of D_s defined by Eq.(2) were 0.13 to 0.17, and were less than half of estimated D_s . Consequently, estimation by Eq.(5) is conservative enough for cylindrical shells with openings.

6 CONCLUSION

From the series of dynamic buckling tests for cylindrical shells with openings under seismic loads, the following conclusions were obtained;

1. Buckling for cylindrical shells with openings was caused as ligaments deformed in the radial direction. Deformed shape was observed as ligaments beneath the loading axis were bulged and others were shrunken. Similar buckling mode was shown on each model.
2. Response reduction factor D_s did not affect circumferential opening ratio α , but it did affect loading direction. D_s whose loading direction was opening side was larger than in cases where the loading direction was the loading side. Accordingly, D_s whose loading direction was the opening side should be used for design.
3. The response reduction factor obtained by the tests was less than half the value estimated when calculated by using equations for cylindrical shells without

- openings.
4. Above all, the concept of reduction factor proposed for cylinders without opening is also applicable for cylindrical shells with openings.

ACKNOWLEDGMENT

This study was carried out as part of a project by the Ministry of International Trade and Industry, titled "Verification Tests of Fast Breeder Reactor Technology", which has been conducted since 1987. Authors gratefully acknowledge the helpful discussions with Prof. H. Akiyama, Prof. H. Ohtsubo (University of Tokyo), Prof. M. Yamada (Tohoku University) and members of the Buckling Committee throughout the course of this work.

REFERENCES

1. Akiyama, H., Ohtsubo, H., Yamada, M., Nakamura, H., Matsuura, S., Hagiwara, Y., Yuhara, T., Hirayama, H., Nakagawa, M. & Ooka, Y. 1995. Outline of the seismic buckling design guideline of FBR main vessels.
SMiRT-13 Vol. I: 445-456
2. Takakura, K., Ueta, M., Dousaki, K., Hayashi, M., Wada, H., Hirayama, H., Ozaki, H. & Ogiso, S. 1993. Improvement of elevated temperature structural design: guide for DFBR in Japan.
SMiRT-12 Vol. E: 77-88

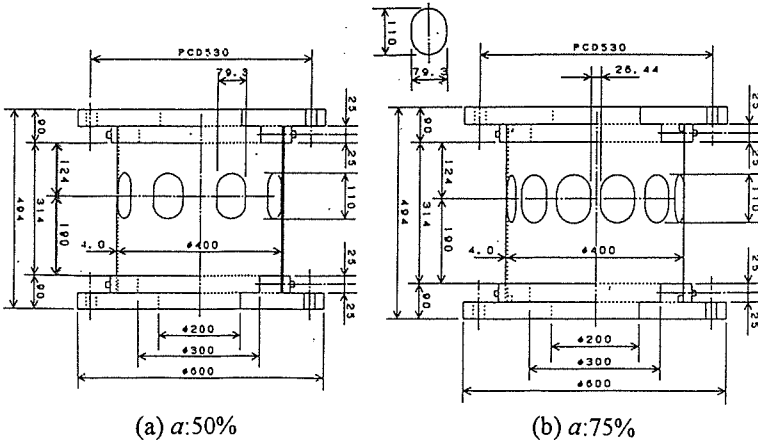


Fig.1 Test model

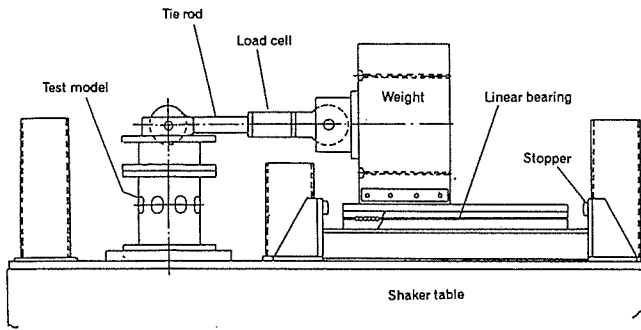


Fig.2 Setup for dynamic test

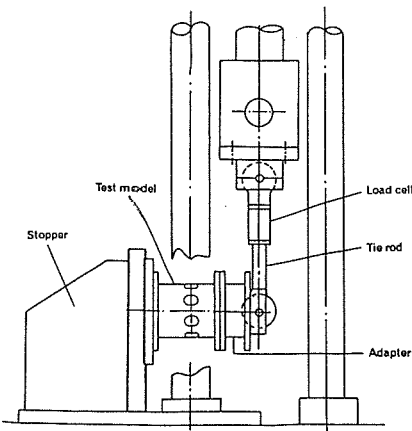


Fig.3 Setup for static test

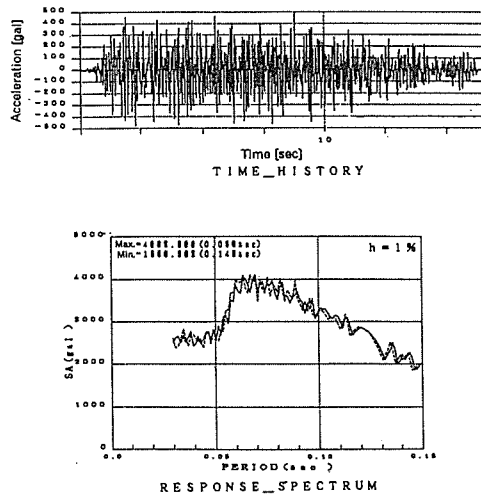


Fig.4 Input acceleration time history and response spectrum

Table 1 Conditions for buckling tests

No.	Radius R [mm]	Circumferential opening ratio α [%]	thickness t [mm]	H/R	Direction of loads	Acceleration of loads [gal]
1-0	200	50	4	2.5	Ligament side	static
1-1						30 ~ 1000
1-2						30, 60, 850
1-3		30, 60, 1100				
2-0		50			Opening side	static
2-1						30 ~ 800
2-2	30, 60, 750					
2-3	30, 60, 850					
3-0	75	Ligament side	static			
3-1			20 ~ 440			
3-2			20, 40, 450			
3-3			20, 40, 500			

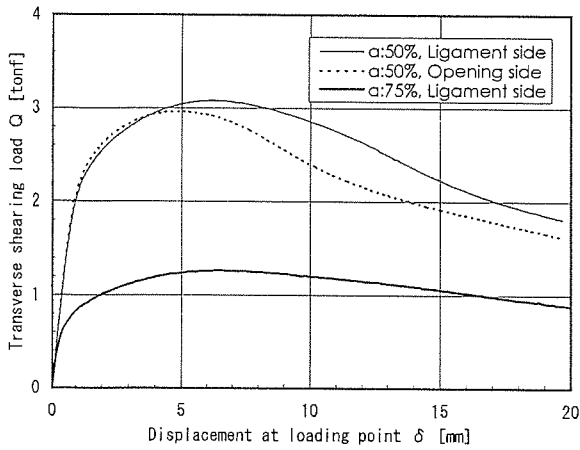
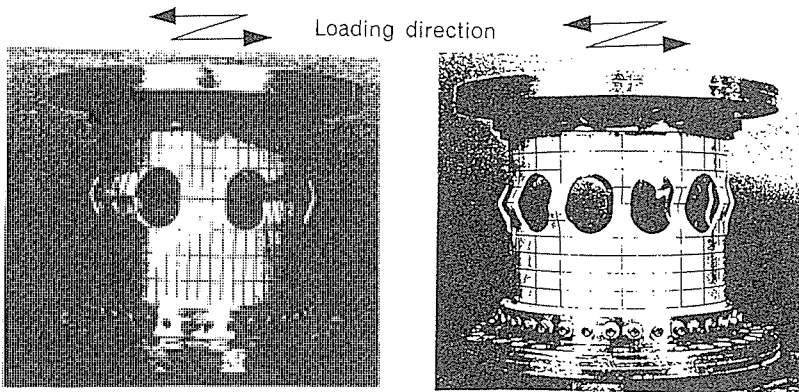


Fig.5 Load-displacement curve under static loads



(a) α :50%, Ligament side

(b) α :75%, Ligament side

Fig.6 Deformation after buckling test under repeated static loads

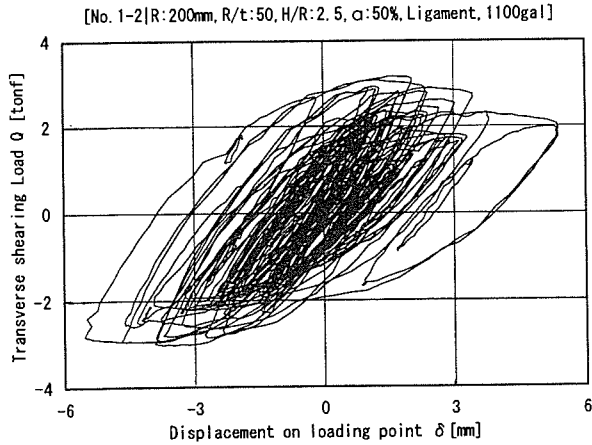


Fig.7 An example of load-displacement curve under seismic loads

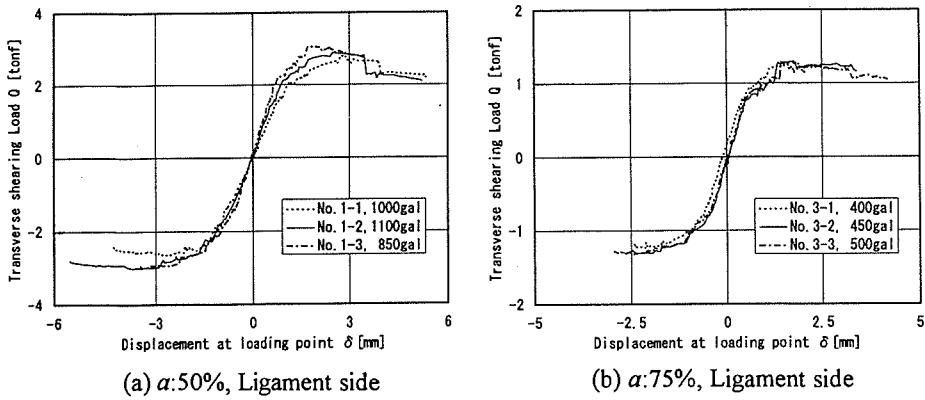


Fig.8 Skeleton curves under seismic loads

Table 2 Buckling load values obtained by dynamic and static tests

No.	Circumferential opening ratio α [%]	Direction of loads	Buckling load Q_{cr}	
			Dynamic test	Static test
1-2	50	Ligament side	3.02	3.08
1-3			3.00	
Ave.			3.01	
2-2	50	Opening side	2.91	2.96
2-3			2.82	
Ave.			2.87	
3-2	75	Ligament side	1.31	1.27
3-3			1.33	
Ave.			1.32	

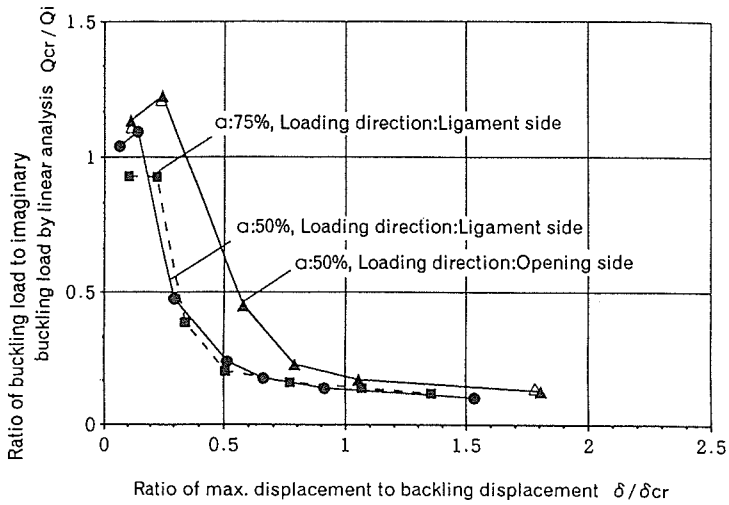


Fig.9 Relations between Q_{cr} / Q_i and δ / δ_{cr} under seismic loads

Table 3 Response reduction factor obtained by test and estimation

Circumferential opening ratio α [%]	Direction of loads	Response reduction factor D_s	
		Test	Estimation
50	Ligament side	0.13	0.45
50	Opening side	0.18	0.45
75	Ligament side	0.14	0.45